Journal of Mechatronics, Electrical Power, and Vehicular Technology 15 (2024) 119-131

Journal of Mechatronics, Electrical Power, and Vehicular Technology

e-ISSN: 2088-6985
p-ISSN: 2087-3379

mev.brin.go.id

Development of styrene butadiene rubber-butadiene rubber with a hyperelastic model for vehicle tire design

Angki Apriliandi Rachmat [a, b], Muhammad Hisyam Ramadhan [c], Yati Mardiyati [c, *], I Wayan Suweca [d], Tatacipta Dirgantara [e]

[a] *Doctoral Program, Faculty of Mechanical and Aerospace Engineering, Institut Teknologi Bandung*
Ganesha 10, Bandung, 40132, Indonesia
[b] *Mechanical Engineering Department, Politeknik Negeri Bandung*
Geger kalong hilir, Bandung Barat, 40559, Indonesia
[c] *Materials Science and Engineering Research Group, Faculty of Mechanical and Aerospace Engineering, Institut Teknologi Bandung*
Ganesha 10, Bandung, 40132, Indonesia
[d] *Engineering Design and Production Research Group, Faculty of Mechanical and Aerospace Engineering, Institut Teknologi Bandung*
Ganesha 10, Bandung, 40132, Indonesia
[e] *Solid Mechanics and Lightweight Structures Research Group, Faculty of Mechanical and Aerospace Engineering, Institut Teknologi Bandung*
Ganesha 10, Bandung, 40132, Indonesia

Abstract

This paper proposes a mathematical correlation between styrene butadiene rubber (SBR)-butadiene rubber (BR) composition and hyperelastic model parameters for numerical studies in vehicle tire design. Experimental, numerical, and curve-fitting methods were employed in this research. Experimental tests were conducted using tensile tests for SBR-BR. The numerical study of the SBR-BR tensile test was carried out using several classic hyperelastic models. The best hyperelastic model was selected based on the smallest deviation between numerical and experimental results. Curve-fitting was done between the best hyperelastic model parameters and the compound to obtain a new correlation, and it was validated. This research shows that the neo-Hookean model with 6 % deviation is the most suitable for the SBR-BR, and the mathematical correlation for SBR-BR composition and C_{10} is linearly correlated. SBR60 %-BR40 % shows the optimum composition for non-pneumatic tires with the characteristic of maximum tensile strength 16.71 MPa, elongation 251 %, and 200 % modulus 13.04 MPa.

Keywords: mathematical correlation; styrene butadiene rubber; butadiene rubber; hyperelastic model; vehicle tire.

* Corresponding Author. mardiyati@itb.ac.id (Y. Mardiyati)

https://doi.org/10.55981/j.mev.2025.1201

Received 14 April 2025; revised 9 May 2025; accepted 11 May 2025; available online 31 July 2025; published 31 July 2025

How to Cite: A. A. Rachmat *et al.*, "Development of styrene butadiene rubber - butadiene rubber with a hyperelastic model for vehicle tire design," *Journal of Mechatronics, Electrical Power, and Vehicular Technology*, vol. 16, no. 1, pp. 119-131, July, 2025.

I. Introduction

Styrene-butadiene rubber (SBR) and butadiene rubber (BR) are the world's second and third-most-used rubber materials. SBR-BR combined with filler and additives produces rubber with specific characteristics [1]. Globally, more than 74 % of SBR is utilized in vehicle tire production [2], with three billion tires manufactured in 2019 [3]. Vehicle tires can be classified as pneumatic and non-pneumatic [4]. The non-pneumatic tire (NPT) or airless tire has one-third of the market size compared to a pneumatic tire. However, it has a compound annual growth rate (CAGR) of 6 % in the forecast 2024-2030 period [5], indicating an increase in demand in the future. Driving safety was also the main issue for non-pneumatic tire development [4][6]. The non-pneumatic tire consists of a compound, frame, and support. SBR base rubber and carbon black filler were commonly used for the non-pneumatic tire [4]. SBR for track vehicle rubber compound (heavy vehicle tire) has been patented and widely used in the United States due to its lower cost and availability [7]. To increase the rubber abrasion resistance, in order to prevent a reduction in vehicle speed [8], a combination of SBR with natural rubber and SBR with polybutadiene can be used [9]. The use of difunctionalized styrene butadiene rubber (DF SBR) enabled the green tires production with low energy consumption [10]. Testing on track pads using a full-scale vehicle has been carried out [11]. It required a complex test setting, various sensors, and a high cost. In advance, the rubber products are made using high-precision molds and large press machines [12]. Thus, vast amounts of materials and long tests are required to obtain the optimum formulation of tire compounds. In order to reduce the amounts of materials used and the time for testing, alternative methods to develop new rubber compounds should be considered. One of the alternative methods is developing a correlation between rubber composition, in this context SBR-BR, and its related parameters using numerical methods.

The numerical method is one method to reduce rubber products' cost and trial time. Many numerical studies were carried out using the uniaxial experimental test method on rubber specimens, and then a hyperelastic model was selected by fitting it with experimental data with regard to hydroplaning effects on motorcycle tires [13], automobile tire side walls application [14], and damage materials [15]. A good agreement between the uniaxial and biaxial tests was reported from a study of the characteristics of the hyperelastic method [16]. Even the uniaxial test showed a better result compared to the planar test using rethreaded truck tire material [17]. This result was also supported by the compression test on O-ring specimens, in which the uniaxial tensile test shows a consistent result compared to the compression test [18]. Therefore, the uniaxial test can be used to represent the compression test. The uniaxial test is more appropriate for hyperelastic neo-Hookean, Yeoh, and first-order Ogden models. Meanwhile, the biaxial test is more suitable for Mooney-Rivlin and second or third-order Ogden. In contrast, a planar test is unnecessary to obtain hyperelastic model parameters with the strain energy density approach [19].

Several hyperelastic models in numerical studies of rubber products show varied results. A non-pneumatic tire study used Mooney-Rivlin and neo-Hookean hyperelastic models for the analysis [6]. For rubber made from tea seed oils for automobile tire side walls, the most suitable models are hyperelastic models Arruda-Boyce, Mooney-Rivlin nine parameters, third-order polynomial, and third-order Yeoh [14]. The Mooney-Rivlin two-parameter model is the closest to the experimental test results for the hyperelastic propellant rubber-like material [16]. In a study on re-treaded tire rubber using numerical methods, the most stable models were provided by the Yeoh and Arruda-Boyce models [17].

Hyperelastic numerical modelling in SBR-BR must consider the correction factor of the Mullins effect, as mentioned by Fazekas and Goda [20] and Zhang *et al.* [21]. Mullins' effect value of r=1.01, m=0.908, and β=0 was used in a study of constitutive modelling of rubbers [20]. Meanwhile, Mullins' effect parameters of r=1.5, m=0.2, and β=0.2 were used in a study of the Mullins effect of rubber materials using the spherical indentation method [21]. Some characteristics of SBR rubber that have been tested with numerical methods were reported in several studies [22] [23]. Numerical and experimental studies of 50 % solution-styrene butadiene rubber (s-SBR) show a better performance in reducing the energy dissipation effect than emulsion-styrene butadiene rubber (e-SBR) [22]. In addition, numerical studies of tank track pads made of SBR and NR compounds at temperatures above 75 °C showed a decrease in tensile strength of 60 %-90 % [23]. There are 85 hyperelastic models divided into phenomenological models and micromechanical network models. Some models are widely used in the phenomenological model category: Mooney-Rivlin, neo-Hookean, Yeoh, and Ogden [24]. Numerical methods verified by experimental tests in vehicle research are widely used, such as in vehicle accident simulations [25].

A correlation between rubber composition and hyperelastic model parameters can be developed to

simplify the process of rubber compounding and vehicle tire design. The classical numerical methods that rely on experimental tensile test data, such as those employed by Ihueze [14], Rajesh [16], and Gudsoorkar [17], are no longer required. The parameters and rubber compound composition can be plotted in a graph and then curved-fitting to obtain a proper correlation. This paper proposed a new mathematical correlation between the SBR-BR base rubber composition and the hyperelastic model, which has not been worked together by other researchers yet. From the mathematical correlation, the tensile strength, strain at break, and 200 % modulus values of SBR-BR rubber for vehicle tires can be easily calculated.

II. Materials and Methods

The research was conducted using experimental and numerical methods. The experimental method started with producing the SBR-BR rubber compound, vulcanization, specimen preparation, and tensile testing. Tensile test results data were then used as input to a numerical study, from which the hyperelastic model that best fits the test data can be obtained. A correlation between the two parameters can be developed by plotting the composition of SBR-BR rubber compound as a function of hyperelastic model parameters.

A. Experimental test

The experimental test consists of three stages: specimen preparation, tensile strength test, and data analysis. This stage was carried out to obtain stress and strain data from the SBR-BR rubber compound. Stress and strain data were used for material input in numerical studies. The specimen preparation stage begins with the process of weighing each ingredient, which also accommodates non-pneumatic tire or heavy vehicle tire applications. The materials used are SBR-BR rubber, filler, and additives. The SBR-BR rubber compound was varied into four base rubbers, namely SBR 100 %-BR 0 % (SB0), SBR 60 %-BR 40 % (SB4), SBR 40 %-BR 60 % (SB6), and SBR 0 %-BR 100 % (SB10). Carbon black N220, widely used by the rubber industry [26] was used as filler in this research. 60 phr carbon black represents the optimum value [27], exceeding this concentration, particle agglomeration tends to occur due to inadequate dispersion. Moreover, the additives are used zinc oxide (ZnO), stearic acid, tetramethyl thiuram disulphide (TMTD), 2,2-methylene bis (4-methyl-6-tert-butylphenol) (BKF), N-cyclohexyl-2-benzothiazole sulfenamide (CBS), and sulfur, as reported by Amin [28]. Other additives for preparing specimens are shown in Table 1, in which each compound specimen was made in 100 grams. A double-roll mill machine X(S)K 160 from Nanjing Co. Ltd with a roller speed of 14 rpm was then used to blend all ingredients for approximately 120 minutes until they were evenly blended. The resulting compound was exposed to air for 24 hours until it reached room temperature [29]. The SBR-BR compound was tested with a rheometer MDR 2000 Alpha to obtain each rubber composition's curing time value (t90).

The rubber compound was vulcanized at 150 °C with an optimum curing time of t90. Rubber vulcanization was carried out at the same time as molding the shape of the tensile test specimen. The standard shape and dimensions of tensile test specimens according to ASTM D412 11 [30], and also consider ISO 527-1 which used by Bylina, 2024 [31], is

Table 1.
Rubber compound material composition.

Rubber composition	Materials	SB0		SB4		SB6		SB10	
		(phr)	(g)	(phr)	(g)	(phr)	(g)	(phr)	(g)
Base rubber A	SBR	100	51.8	60	31.1	40	20.7	0	0.0
Base rubber B	BR	0	0.0	40	20.7	60	31.1	100	51.8
Activator	ZnO	5	2.6	5	2.6	5	2.6	5	2.6
	Stearic acid	2	1.0	2	1.0	2	1.0	2	1.0
Filler	N220	65	33.7	65	33.7	65	33.7	65	33.7
Reinforcing resin	Rhenosin A (phenolic)	5	2.6	5	2.6	5	2.6	5	2.6
Dispersion resin	Rhenosin 145AP	3	1.6	3	1.6	3	1.6	3	1.6
	Rhenosin GE	3	1.6	3	1.6	3	1.6	3	1.6
Anti-degradant	Vulkanox TMQ	2	1.0	2	1.0	2	1.0	2	1.0
	Vulkanox 4010	2	1.0	2	1.0	2	1.0	2	1.0
	Antilux Wax	2	1.0	2	1.0	2	1.0	2	1.0
Curing	TBBS	2	1.0	2	1.0	2	1.0	2	1.0
	Sulfur	2	1.0	2	1.0	2	1.0	2	1.0

shown in Figure 1. The dimension is shown in Figure 1(a). Each specimen composition was made from a minimum of five specimens as shown in Figure 1(b).

Tensile strength tests were carried out on rubber specimens SB0, SB4, SB6, and SB10 with the Instron 6800 universal tensile machine. The specimen was clamped on a section with a width of 16 mm. Pneumatic clamping is a good method for conducting uniaxial tests [32]. The parameter being controlled was elongation at a 500 mm/min extension rate, and the specimens were pulled until failure occurred. The desired results are the force and elongation of rubber specimens and the time for the specimen to break. Force and elongation data were then processed into engineering stress and strain as input for the numerical study of materials. Specimen break time was also used as one of the numerical study parameters.

B. Numerical study

The numerical study was carried out by following the experimental test specimen model is shown in Figure 2. The general step is shown in Figure 2(a). The stages of the numerical review using Abaqus are defining the material, analysing the hyperelastic model, modelling the specimen, meshing the model, determining boundary conditions, and applying load as shown in Figure 2(b), and also conducting analysis from Figure 2(c). This stage was carried out to determine the most suitable hyperelastic model for the SBR-BR rubber compound and the hyperelastic model parameter values for each rubber composition. The best hyperelastic model was selected from the smallest deviation value between the tensile strength resulting from numerical studies and experimental tests.

The material used in the numerical study was defined as a hyperelastic material with stress and strain data input from experimental test results of SB0, SB4, SB6, and SB10. The mass density and the Mullins effect parameter were also described at the materials stage. The numerical reviews are continued by analysing energy stability in several hyperelastic models: Mooney-Rivlin, neo-Hookean, Yeoh, Ogden, polynomial, Arruda-Boyce, and reduced polynomial. equation 1 to equation 5, those used by Abaqus, are general equations of strain energy deformation for the phenomenological theory for an incompressible, isotropic, and hyperelastic material. They were expressed in terms of the coefficients and the invariants of the left or right Cauchy-Green deformation tensor [19]. After material analysis, the research continued with experimental test modelling.

$$W = \sum_{i,j=0}^{\infty} C_{ij}(I_1 - 3)^i (I_2 - 3)^j \quad (1)$$

where Ii are I_1, I_2, and I_3,

$$I_1 = {\lambda_1}^2 + {\lambda_2}^2 + {\lambda_3}^2$$

$$I_2 = {\lambda_1}^2{\lambda_2}^2 + {\lambda_2}^2{\lambda_3}^2 + {\lambda_1}^2{\lambda_3}^2$$

$$I_3 = {\lambda_1}^2{\lambda_2}^2{\lambda_3}^2$$

For neo-Hookean,

$$W = C_{10}(I_1 - 3) \quad (2)$$

For Mooney-Rivlin,

$$W = C_{10}(I_1 - 3) + C_{01}(I_2 - 3) \quad (3)$$

For Yeoh,

$$W = C_{10}(I_1 - 3) + C_{20}(I_1 - 3)^2 + C_{30}(I_1 - 3)^3 \quad (4)$$

For Ogden,

$$W = \sum_{i=1}^{\infty} \frac{\mu_i}{\alpha_i}({\lambda_1}^{\alpha_i} + {\lambda_2}^{\alpha_i} + {\lambda_3}^{\alpha_i} - 3) \quad (5)$$

where W is strain energy deformation, C_{ij} is coefficients of incompressible, isotropic, and hyperelastic material, I_i is invariants of the left or right Cauchy-Green deformation tensor, λ is principal extension ratios, μ_i is shear modulus, α_i is Ogden exponent.

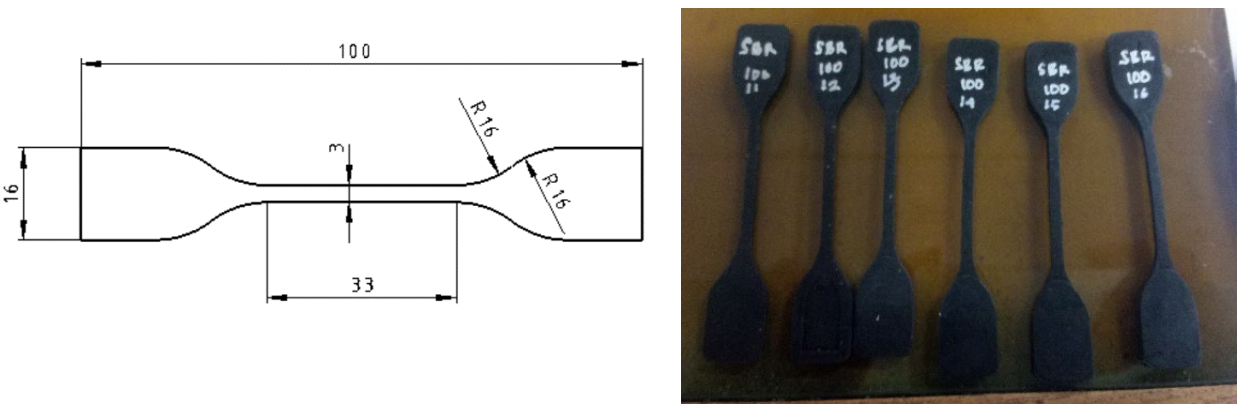

(a) (b)

Figure 1. Vulcanized rubber specimen based on ASTM D412 dies D. (a) dimensions; (b) mold result.

Specimen modelling starts with making a 3D model of the tensile test specimen. The dimensions of the specimen in the numerical study are the same as those used in the experimental tests. Then, the 3D model was meshed and divided into several segments to obtain optimum meshing quality. Modelling was continued by determining the boundary conditions. The left end was set at a fixed position, while the right side was given a displacement equal to the maximum elongation in the experimental test. Other important parameters that need to be determined are the test time and the interval for data collection. Once the parameters have been determined, a numerical model could be computed.

The desired numerical study results are reaction forces and displacements from several hyperelastic models for calculating the tensile strength, elongation, and 200 % modulus. The deviation can be determined from the comparison between the experimental data and the tensile strength and 200 % modulus. The model with the smallest deviation was selected as the best hyperelastic model and was used to develop a new equation for the correlation.

C. Analysis

Using the curve-fitting method, the new mathematical correlation can be developed according to the steps depicted in Figure 3. Curve-fitting was performed on the data plot between the rubber compositions SB0, SB4, SB6, and SB10 and the parameters of the best hyperelastic model. A trend line was created to equate the relationship between rubber composition and hyperelastic parameters. The quality

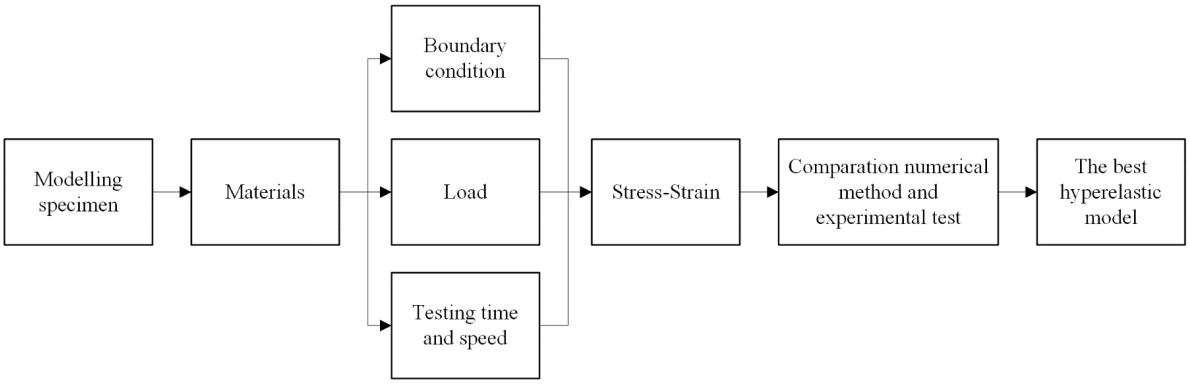

a)

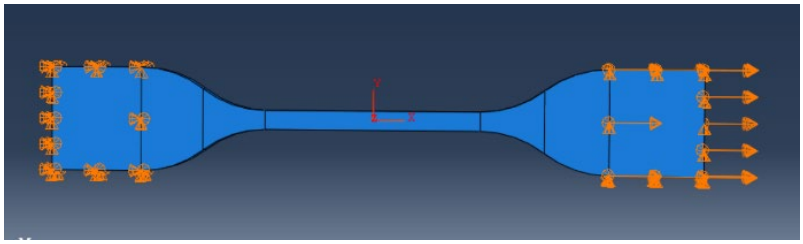

(b)

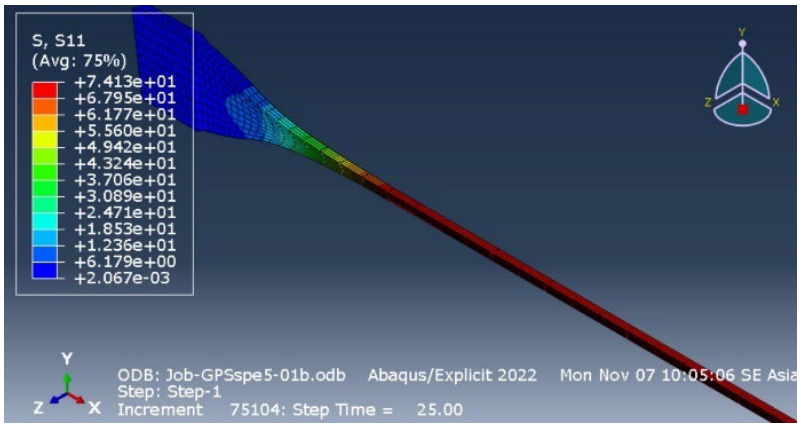

(c)

Figure 2. Numerical method process. (a) general step; (b) boundary conditions and load; (c) result and analysis.

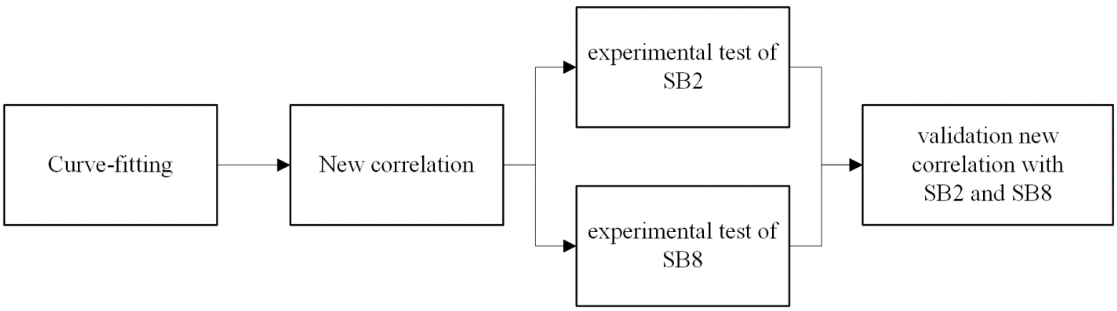

Figure 3. Analysis method process.

of curve-fitting was checked through the correlation coefficient value. Furthermore, the new correlation was validated by experimental tests of different SBR-BR compositions.

The validation of the new correlation was accomplished using experimental tests of 80% SBR-20 % BR (SB2) and 20 % SBR-80 % BR (SB8). It should be noted that SB2 and SB8 were fabricated and tested using a similar method to that in SB0, SB4, SB6, and SB10. Hyperelastic model parameters obtained from the experiment using SB2 and SB8 were compared with those obtained from the new correlation. Model parameters resulting from the SB2 and SB8 experimental tests were compared with the hyperelastic parameters calculated using the mathematical correlation.

III. Results and Discussions

This section discusses the results of the research involving experimental tests, numerical studies, and correlation development. The experimental test results include the stress-strain of every specimen composition. Its characteristics can be used for non-pneumatic tire compounds. From the experimental tests, force-elongation relationships of rubber vulcanization SB0, SB4, SB6, and SB10 are obtained. These data were then processed to obtain stress-strain relations of the compounds, as shown in Figure 4. The tensile strength material characteristic for non-pneumatic tire compound, which can be supported by the SBR-BR composition, is in the range of 13 MPa to 19 MPa with 65 phr carbon black filler. A lower tensile strength in the range of 5.5 MPa – 8.5 MPa was proposed by Fujikawa, *et al.* [33] by using carbon black volume fraction from 10 % to 20 %. This confirms that the tensile strength is proportional to carbon black composition.

From the present work, it is also obvious that the tensile strength of specimens using SB0 and SB4 are higher than that of the ground pad shoe used in medium tanks produced by Pindad Indonesia and FNSS Turkey [34]. Therefore, both specimens can be considered as materials for a ground pad shoe, heavy vehicle tire, or non-pneumatic tire type. The most elastic composition, with around 280 % maximum elongation, was shown in SB0 and SB10. It is 15 % higher than the other compositions. From the experimental test results, all SBR-BR compositions broke out at different stresses. SB0 broke at 2.79 mm/mm, SB4 at 2.38 mm/mm, SB6 at 2.58 mm/mm, and SB10 at 2.63 mm/mm.

Detailed examination of Figure 4 reveals that the most significant effect of strain on the stress is found for SB4. It is also clear that in the range of strain from 0 to 0.5, the effect of strain on the stress is almost identical for all specimens. Starting from the strain of 0.5, the effect of strain on the stress of all specimens can be clearly distinguished. SB4 has a slope of 7.65 MPa, higher than that of SB0 (7.63), SB6 (5.53), and SB10 (5.3). The slope for SB4 is 0.3%, 28 %, and 32 % higher than that of SB0, SB6, and SB10, respectively. Figure 5. shows the maximum tensile strength, strain at break, and 200 % modulus obtained from the experiments. The 200 % modulus of SB0, SB4, SB6, and SB10 are 12.36 MPa, 13.04 MPa, 10.46 MPa, and 10.07 MPa, respectively. This parameter is significantly higher than those of tank M-60 (4 MPa) and counter obstacle vehicle (5.4 MPa) as reported in a patent number US5264290A [35].

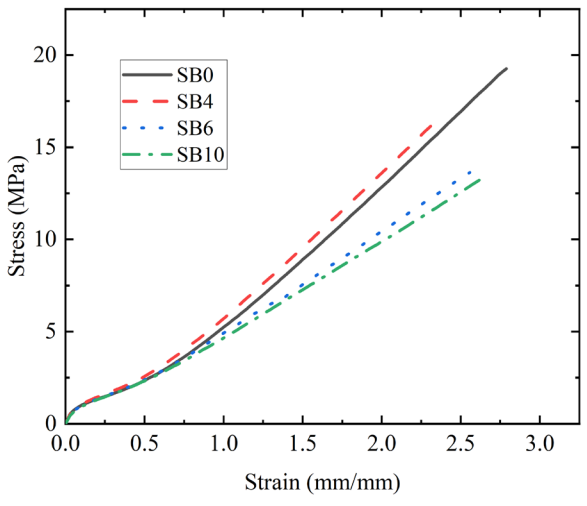

Figure 4. Stress-strain experimental test results.

The maximum standard deviation of the experiment is 0.71 for tensile strength, 0.2 for strain at break, and 1.06 for 200 % modulus. The low standard deviation indicates that the experiment has good repeatability. The highest tensile strength of the rubber blend is obtained from SB0, with a value of 19.38 MPa. Adding BR causes a decrease in tensile strength and strain at break, this phenomenon is in agreement with the findings reported in the Sae-oui study [36]. However, the strain at break was slightly increased in SB10. In addition, there was an increase in the 200 % modulus with the addition of BR content, where the optimum compound was SB4. The 200 % modulus after SB4 is decreased significantly due to the uniqueness of the SBR - BR combination.

The hyperelastic model that best fits the experimental data was desired in the numerical study. To determine the best model, nine models were evaluated, i.e., Mooney-Rivlin, second-order polynomial, first-order Ogden, second-order Ogden, third-order Ogden, neo-Hookean, second-order reduced polynomial, Yeoh, and Arruda-Boyce. Five models show stability for numerical studies: second-order polynomial, first-order Ogden, neo-Hookean, second-order reduced polynomial, and Arruda-Boyce. A time step parameter of 40 was used to set the amplitude value during loading from zero to maximum. In addition, the Mullins effects parameters of r=1.5, m=0.2, and β=0.2 were used.

The results of the numerical study of each selected hyperelastic model are shown in Figure 6. These charts are the result of the second-order polynomial, first-order Ogden, neo-Hookean, and Arruda-Boyce methods. All charts show a trend of decreasing tensile strength values along with the addition of BR, except for the second-order reduced polynomial, which shows the same trend as the experimental study in Figure 4. Stress values at strains of less than 0.5 indicate unstable results. However, the instability of the graph is not a problem because the characteristic used is the maximum tensile strength value located at a strain value above 2.5. The maximum stress from the

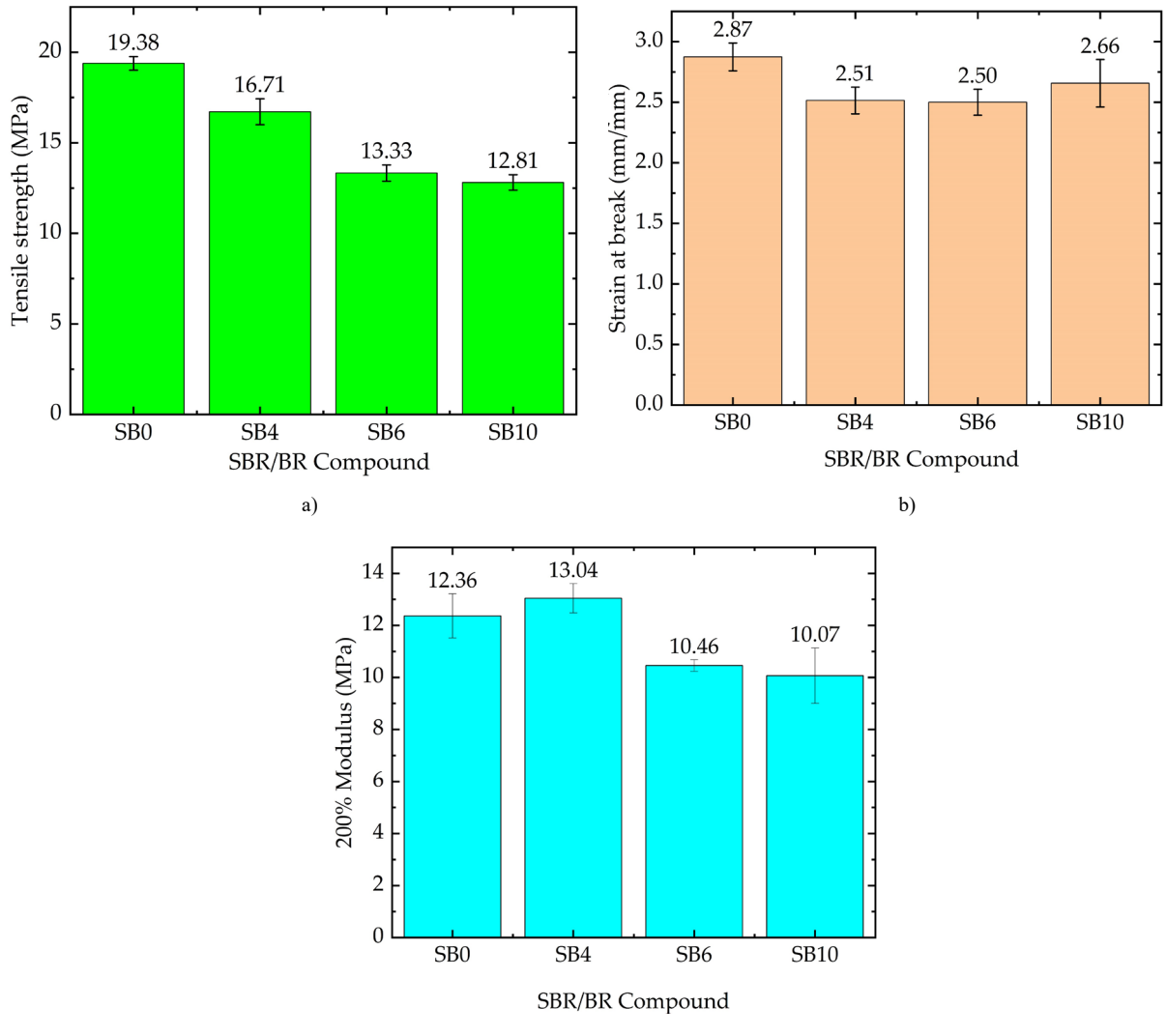

Figure 5. Experimental test results of SBR-BR compound. a) Maximum tensile strength; b) Strain at break; c) 200 % modulus.

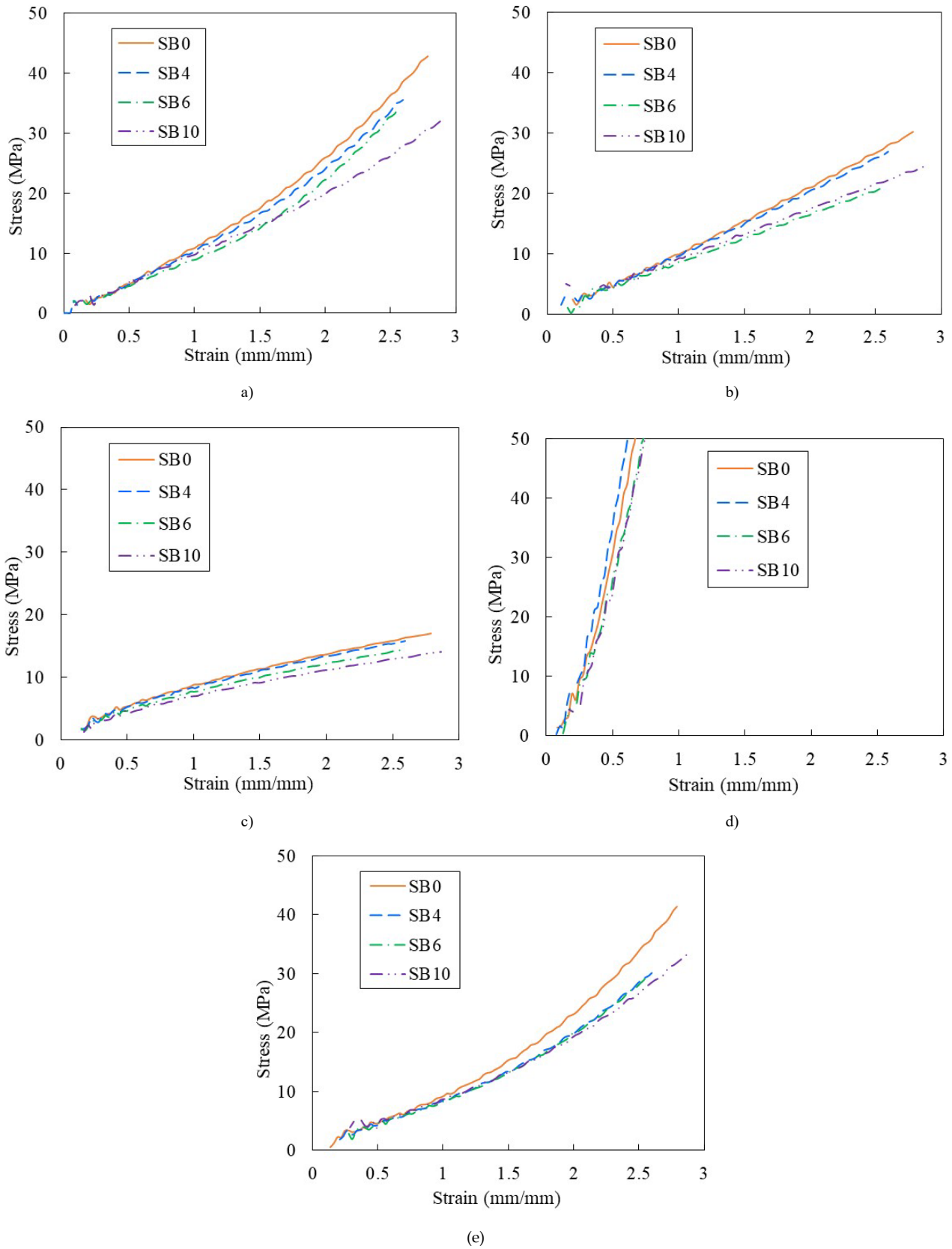

Figure 6. Numerical results of SBR-BR. a) second-order Polynomial; b) first-order Ogden; c) neo-Hookean, d) second-order reduce-Polynomial; e) Arruda-Boyce.

numerical study ranges from 20 MPa to 500 MPa. The neo-Hookean method shows the smallest stress in 20 MPa, Ogden shows 30 MPa, Arruda-Boyce and Polynomial show 45 MPa, and the highest stress is shown by reduced-polynomial at 500 MPa. As seen from the charts, the neo-Hookean model in Figure 6(a) shows a polynomial form that approaches linear with the R-squares (correlation coefficient) for the polynomial is 99 % and the linear 97 %. The first-order Ogden model in Figure 6(b) shows a linear trend with

an R-squared value of 99 %. Figure 6(c) and Figure 6(d) for the Arruda-Boyce and second-order polynomial models show a similar trend in the polynomial's shape that opens upwards approaching linear. Both of these charts have a second-order polynomial R-squared of 99 % and linear R-squared of 96 % and 98 %. For the three models of first-order Ogden, Arruda-Boyce, and second-order polynomial, the maximum stress value is twice compared to that of the neo-Hookean model. The last model, i.e., the second-order reduced polynomial in Figure 6(e), shows the highest stress, up to 500 MPa. This is about 25 times higher than that of neo-Hookean. Instead of SB0, the highest stress value is obtained by SB4, as obtained by the experimental test.

The result of the numerical study is plotted based on SBR-BR compositions. Compared to the experimental test, the neo-Hookean hyperelastic model shows the closest result with a maximum tensile strength average deviation of 6%. The overall neo-Hookean deviation of all SBR-BR compositions were SB0 = 12%, SB4 = 6%, SB6 = 7%, and SB10 = 0%. From the distribution of the deviation values, the neo-Hookean model has a standard deviation value of 4 MPa. The standard deviation of the other numerical model deviation in sequence was first-order Ogden value 12 MPa, Arruda-Boyce 26 MPa, second-order polynomial 16 MPa, and second-order reduced polynomial very large. From these values, the results of the numerical study using neo-Hookean are similar to the experimental test results. The unfit graphics at 100% elongation are neglected according to each model hyperelastic original characteristics from the Abaqus, this model does not modify. The original model will make the other user rework this research result. A graphical comparison of experimental and numerical study results can be seen in Figure 7.

The neo-Hookean parameter (C_{10}) was used to create mathematical correlations with the SBR - BR rubber compound. C_{10} of each SBR-BR compound (100 %-0 %, 60 %-40 %, 40 %-60 %, 0 %-100 %) was plotted on a single graph, as shown in Figure 8. Detailed inspection of Figure 8 reveals that the neo-Hookean parameter has an almost linear relationship with the composition of SBR-BR. The relation coefficient or

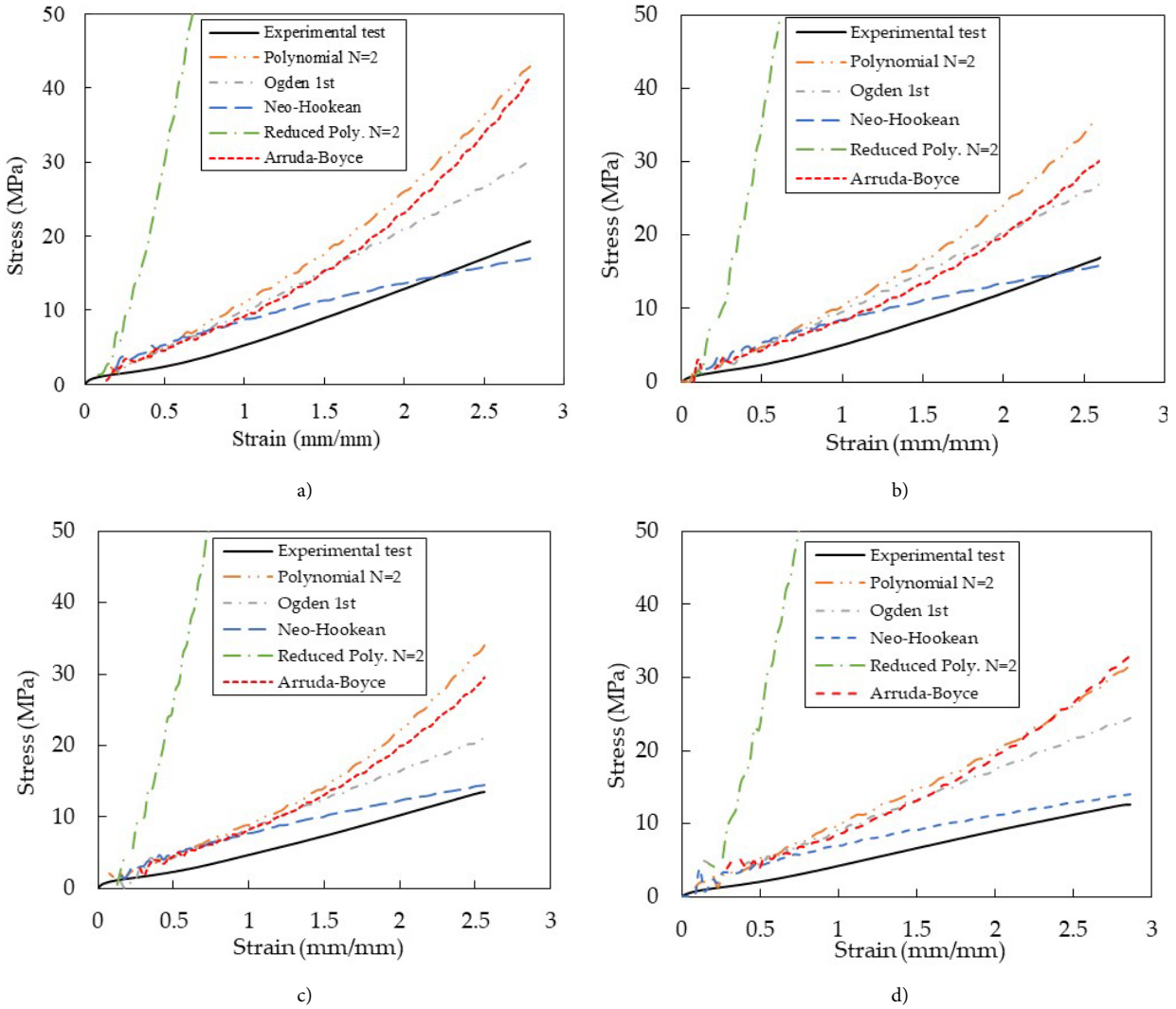

Figure 7. Stress-strain comparison between numerical and experimental tests. a) SB0; b) SB4; c) SB6; d) SB10.

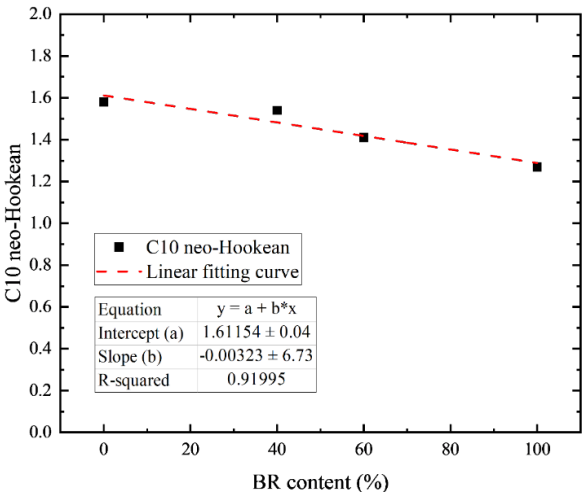

Figure 8. SBR-BR relation to the hyperelastic model parameter.

R-squared of the SBR-BR curve-fitting showed a good result with 92 %. It means that the SBR-BR composition has a strong linear correlation with the C_{10} neo-Hookean parameter. SBR-BR composition in this equation means the percentage of BR content (%) in the 100 % SBR-BR composition. The relationship can be expressed as equation (6).

$$y = -0.0032x + 1{,}61 \quad (6)$$

The negative coefficient of equation (6) implies a decrease of the neo-Hookean parameter with the increase of BR content in the SBR-BR blend. In other words, the increase of BR content in the SBR-BR blend causes the decrease of tensile strength and elongation at break. Every additional 10 % BR rubber causes a 0.032 decrease in the C_{10} neo-Hookean parameter. Overall value of C_{10} neo-Hookean parameter of SBR-BR composition from 0 %-100 % is 1.61 – 1.29. This new mathematical correlation only applies to carbon black filler N220 65 phr and additives, as summarized in Table 1.

The validation of the mathematical correlations with experimental tests using SB2 and SB8 shows a less than 5 % deviation. Validation using SB2 resulted in the C_{10} value from the mathematical correlation of 1.55. From the experiment, the C_{10} value is 1.49, resulting in a deviation of 4 %. In the second validation using SB8, a C_{10} value of 1.35 resulted from the mathematical correlation and 1.38 from the experiment, and produced a deviation of 2 %. The validation of the mathematical correlation is summarized in Table 2. The next steps of validation were the comparison of maximum tensile strength, strain at break, and 200 % modulus values between the mathematical correlation and experimental tests. The graphics comparison is plotted in Figure 9, showing that the maximum stress is nearly identical. The significant difference at 50 %-150 % of maximum elongation will not influence the tensile strength characteristic for the compound because the needed characteristic is the maximum tensile strength, which is calculated based on the maximum stress. The phenomenological type of hyperelastic model should be the causative factor. Validation tensile strength value using SB2 and SB8 shows the maximum deviation is 8 % and 6 %, respectively, as shown in Table 3. These deviations are less than 10 %, indicating a good correlation. The deviation of strain at break is zero, as presented in Table 4, because the load is applied based on displacement data from the experiment, resulting in consistent outcomes. As shown in Table 5, the deviation of the 200 % modulus value is 8 % and 17 %. These results are quite unique and interesting in future research. Overall, the validation shows that the deviation of tensile strength and strain at break is less than 10 %, except for the 200 % modulus at 20 % SBR, which is 17 %. It means that the mathematical correlation can represent experimental tests of maximum tensile strength, strain at break, and 200 % modulus of SBR/BR rubber compounds.

From previous discussions, it was revealed that the new mathematical correlation in this study can be used for obtaining the material characteristics of the SBR-BR compound without conducting rubber compounding

Table 2.
New mathematical correlations validation by C_{10}.

Variations	C_{10}		Deviation (%)
	New correlation	Experimental test	
SB2	1.55	1.49	4
SB8	1.35	1.38	2

Table 3.
New mathematical correlations validation by maximum tensile strength.

Variations	Max tensile strength (MPa)		Deviation (%)
	New correlation	Experimental test	
SB2	15.58	16.96	8
SB8	13.99	13.14	6

Table 4.
New mathematical correlations validation by strain at break.

Variations	Strain at break (mm/mm)		Deviation (%)
	New correlation	Experimental test	
SB2	2.65	2.65	0
SB8	2.52	2.52	0

Table 5.
New mathematical correlations validation by 200 % modulus.

Variations	Strain at break (mm/mm)		Deviation (%)
	New correlation	Experimental test	
SB2	12.88	11.88	8
SB8	11.998	10.25	17

and tensile testing. Using equation (6), the C_{10} neo-Hookean parameter can be determined and inputted to Abaqus software to obtain maximum tensile strength, strain at break, and 200 % modulus values. The results from this research can be used as a complement to the existing rubber research and hyperelastic model research.

IV. Conclusion

The highest tensile strength of the rubber blend is obtained from SB0, with a value of 19.38 MPa. Adding BR causes a decrease in tensile strength and strain at break. However, the strain at break was slightly increased in SB10. In addition, there was an increase in the 200 % modulus with the addition of BR content, where the optimum compound was SB4. A mathematical correlation of SBR-BR and the hyperelastic model parameter of the vehicle tire equation design was successfully developed. The hyperelastic model of neo-Hookean was introduced to build a new mathematical correlation. The mathematical correlation is y=-0.0032x+1.61, where x is the BR content (%) at SBR-BR rubber compound of the tire, and y is the C_{10} neo-Hookean hyperelastic model. Therefore, without conducting laboratory tests, this equation is able to calculate tensile strength, elongation, and 200 % modulus data for the SBR-BR rubber compound. From this equation, it also reveals that the coefficient of the neo-Hookean model for SBR-BR is in the range of 1.29 (0 % SBR) to 1.61 (100 % SBR). Research development in this field in the future is still widely open. In addition, the research method in this study can be utilized to obtain new correlations for other rubber and vehicle tire types. In the near future, the coefficients for the hyperelastic model are highly demanded to obtain the tensile strength, elongation at break, 200 % modulus, tear strength, and abrasive strength for various rubber types.

Declarations

Author contribution

A.R. Rachmat: Writing - Original Draft, Writing - Review & Editing, Conceptualization, Experimental Testing, Formal Analysis, Visualization. **M. H. Ramadhan**: Draft Review & Editing, Experimental Testing. **Y. Mardiyati, I W. Suweca**: Draft Review, Analysis, Supervision. **T. Dirgantara:** Supervision.

Funding statement

Indonesia Endowment Fund for Education Agency is greatly appreciated for its support funding.

Competing interest

The authors declare that they have no known competing financial interests or personal relationships that could have appeared to influence the work reported in this paper.

Additional information

Reprints and permission: information is available at https://mev.brin.go.id/.

Publisher's Note: National Research and Innovation Agency (BRIN) remains neutral with regard to jurisdictional claims in published maps and institutional affiliations.

References

[1] B. Erman, J. E. Mark, and C. M. Roland, "The Science and Technology of Rubber", 4. ed. *Amsterdam Heidelberg: Elsevier Academic Press*, 2013.

[2] V.M. Il'in and A.K. Rezova, "Styrene Butadiene Rubber: Production Worldwide," *Int. Polym. Sci. Technol.*, vol. 42, no. 10, pp. 35–44, Oct. 2015

[3] Y. Dong, Y. Zhao, U. Hossain, Y. He, and P. Liu, "Life cycle assessment of vehicle tires : A systematic review," *Clean. Environ. Syst.*, vol. 2, no. March, p. 100033, 2021,

[4] Y. Deng, Z. Wang, H. Shen, J. Gong, and Z. Xiao, "A comprehensive review on non-pneumatic tyre research," *Mater. Des.*, vol. 227, p. 111742, 2023,
[5] "Verified market reports," August 2024. Accessed: Aug. 13, 2024. [Online].
[6] Z. Hryciów, J. Jackowski, and M. Żmuda, "The Influence of Non-Pneumatic Tyre Structure on its Operational Properties," *Int. J. Automot. Mech. Eng.*, vol. 17, no. 3, pp. 8168–8178, 2020,
[7] D. P. Flanagan, P. Touchet, and H. O. Feuer, "Elastomers for Tracked Vehicles: 1980-1997 Program to Improve Durability of Rubber Tank Pads for Army Tracked Vehicles," 2015. [Online].
[8] Y. Yunazwin azaruddin, E. Leksono, and Z. Abidin, "Pengembangan Sistem Kontrol Traksi Mobil Elektrik Berbasis Rekonstruksi Keadaan Kecepatan Model Roda," *J. Mechatronics, Electr. Power, Veh. Technol.*, vol. 01, no. 2, pp. 2087–3379, 2010, [Online].
[9] Bergstorm Edward W., "Wear Resistant Rubber Tank Track Pads," 1975. [Online].
[10] Y. Xu, Y. Liu, Y. Gao, L. Liu, and L. Zhang, "Designing high-performance green tire treads by reinforcing the styrene-butadiene rubber/silica interface with chain difunctionalization," *Compos. Part B Eng.*, vol. 290, p. 111887, 2025,
[11] W. Liu, K. Cheng, and J. Wang, "Failure analysis of the rubber track of a tracked transporter," *Adv. Mech. Eng.*, vol. 10, no. 7, pp. 1–8, Jul. 2018,
[12] Z. Zhang, F. Guo, Y. Ke, C. Xiang, and X. Jia, "Effect of vulcanization on deformation behavior of rubber seals: Thermal–mechanical–chemical coupling model, numerical studies, and experimental validation," *Mater. Des.*, vol. 224, Dec. 2022,
[13] P. Meethum and C. Suvanjumrat, "Numerical Study of Dynamic Hydroplaning Effects on Motorcycle Tires," *Int. J. Automot. Mech. Eng.*, vol. 20, no. 1, pp. 10192–10210, 2023,
[14] C. C. Ihueze and C. O. Mgbemena, "Modeling Hyperelastic Behavior of Natural Rubber/Organomodified Kaolin Composites Oleochemically Derived from Tea Seed Oils (Camellia sinensis) for Automobile Tire Side Walls Application," *J. Sci. Res. Reports*, pp. 2528–2542, 2014,
[15] M. Miñano and F. J. Montáns, "A formulation for hyperelastic damaged materials," *Civil-Comp Proc.*, vol. 108, pp. 1–12, 2015,
[16] A. Rajesh, B. Satya Narayana, and K.Sreeramulu, "Characterization of Hyperelastic Material Using Experimental Data and Finite Element Simulation," *Mater. Today Proc.*, vol. 24, pp. 1660–1669, 2020,
[17] U. Gudsoorkar and R. Bindu, "Computer simulation of hyper elastic re-treaded tire rubber with ABAQUS," in *Materials Today: Proceedings, Elsevier Ltd,* 2020, pp. 1992–2001.
[18] B. Yenigun, E. Gkouti, G. Barbaraci, and A. Czekanski, "Identification of Hyperelastic Material Parameters of Elastomers by Reverse Engineering Approach," *Materials* (Basel)., vol. 15, no. 24, Dec. 2022,
[19] X. Li and Y. Wei, "Classic strain energy functions and constitutive tests of rubber-like materials," *Rubber Chem. Technol.*, vol. 88, no. 4, pp. 604–627, Dec. 2015,
[20] B. Fazekas and T. J. Goda, "Constitutive modelling of rubbers: Mullins effect, residual strain, time-temperature dependence," *Int. J. Mech. Sci.*, vol. 210, Nov. 2021,
[21] M. G. Zhang *et al.*, "Investigation on Mullins effect of rubber materials by spherical indentation method," *Forces Mech.*, vol. 4, Oct. 2021,
[22] S. Samaei, M. H. R. Ghoreishy, and G. Naderi, "Effects of SBR molecular structure and filler type on the hyper-viscoelastic behavior of SBR/BR radial tyre tread compounds using a combined numerical/experimental approach," *Iran. J. Polym. Sci. Technol.*, vol. 32, no. 1, pp. 65–78, May 2019,
[23] P. Thavamani, A. K. Bhowmick, and D. Khastgir, "Effect of ageing on strength and wear of tank track pad compounds," *Wear*, vol. 170, no. 1, pp. 25–32, Nov. 1993,
[24] H. He, Q. Zhang, Y. Zhang, J. Chen, L. Zhang, and F. Li, "A comparative study of 85 hyperelastic constitutive models for both unfilled rubber and highly filled rubber nanocomposite material," *Nano Mater. Sci.*, vol. 4, no. 2, pp. 64–82, Jun. 2022,
[25] A. R. Zubir, K. Hudha, and N. H. Amer, "Enhanced Modeling of Crumple zone in Vehicle Crash Simulation Using Modified Kamal model Optimized with Gravitational Search Algorithm," *Automot. Exp.*, vol. 6, no. 2, pp. 372–383, 2023,
[26] Y. Fan, G. D. Fowler, and M. Zhao, "The past, present and future of carbon black as a rubber reinforcing filler – A review," *J. Clean. Prod.*, vol. 247, p. 119115, Feb. 2020,
[27] H. Boukfessa and B. Bezzazi, "The effect of carbon black on the curing and mechanical properties of natural rubber/ acrylonitrile- butadiene rubber composites," *J. Appl. Res. Technol.*, vol. 19, no. 3 SE-Articles, pp. 194–201, Jun. 2021,
[28] L. M. N. Amin, I. Hanafi, and O. Nadras, "Comparative study of Bentonite filled acrylonitrile butadiene rubber and carbon black filled NBR composites properties," *Int. J. Automot. Mech. Eng.*, vol. 15, no. 3, pp. 5468–5475, 2018,
[29] R. Umunakwe *et al.*, "Effect of Varied Cure Temperature on the Cure Behavior, Mechanical Properties and Heat Build-Up of Solid Tire Tread Compound Containing Different Particles Sizes of Ground Tire Rubber," *J. Appl. Sci. Process Eng.*, vol. 11, no. 1, pp. 60–77, 2024,
[30] A. N. Standard, "Standard Test Methods for Vulcanized Rubber and Thermoplastic Elastomers-Tension, ASTM D412," *American Society for Testing and Materials,* Washington, D.C., USA, September 13, 1968. 1969. [Online].
[31] B. Grynkiewicz-Bylina, B. Rakwic, M. Gawlik-Jędrysiak, M. Szymiczek, and B. Chmielnicki, "Methodology for Testing the Uniformity of the Composition of a Batch of Polymer Materials on the Example of Sbr Rubber Granulates in the Aspect of Potential Applications," *Adv. Sci. Technol. Res. J.*, vol. 18, no. 7, pp. 354–363, 2024,
[32] V. Mykhailiuk *et al.*, "Derivation of Material Constants for Experimental SKR-788 Silicone Samples via

Simulation Modeling and Laboratory Testing," *Adv. Sci. Technol. Res. J.*, vol. 18, no. 5, pp. 268–276, 2024,

[33] M. Fujikawa, N. Maeda, J. Yamabe, and M. Koishi, "Performance evaluation of hyperelastic models for carbon-black-filled SBR vulcanizates," *Rubber Chem. Technol.*, vol. 93, no. 1, pp. 142–156, 2020,

[34] A. A. Rachmat, T. Dirgantara, I. W. Suweca, and Y. Mardiyati, "Kaji Numerik Ground Pad Shoe Kendaraan Tempur Dengan Model Material Hyperelastic," *Mesin*, vol. 30, no. 1, pp. 64–74, 2024,

[35] Touchet, Paul *et al.*, "United states patent; 'rubber compound for track vehicle tracks pad,'" 1993 [Online].

[36] P. Sae-oui, K. Suchiva, C. Sirisinha, W. Intiya, P. Yodjun, and U. Thepsuwan, "Effects of Blend Ratio and SBR Type on Properties of Carbon Black-Filled and Silica-Filled SBR/BR Tire Tread Compounds," *Adv. Mater. Sci. Eng.*, vol. 2017, no. 1, p. 2476101, Jan. 2017,